Quaternary International 389 (2015) 213–223

Contents lists available at ScienceDirect

Quaternary International

journal homepage: www.elsevier.com/locate/quaint

Revisiting the ESR chronology of the Early Pleistocene hominin occupation at Vallparadís (Barcelona, Spain)

Mathieu Duval [a, *], Jean-Jacques Bahain [b], Christophe Falguères [b], Joan Garcia [c, d], Verónica Guilarte [a], Rainer Grün [e], Kenneth Martínez [c], Davinia Moreno [b], Qingfeng Shao [f], Pierre Voinchet [b]

[a] Programa de Geocronología, Centro Nacional de Investigación sobre la Evolución Humana, CENIEH, Spain
[b] Muséum National d'histoire Naturelle, Département de Préhistoire, UMR7194 du CNRS, France
[c] URV, Universitat Rovira i Virgili, Àrea de Prehistòria, Avinguda de Catalunya 35, 43002, Tarragona, Spain
[d] UOC, Universitat Oberta de Catalunya (UOC), Avinguda del Tibidabo 39-43, 08035, Barcelona, Spain
[e] Research School of Earth Sciences, The Australian National University, Australia
[f] Nanjing Normal University, College of Geography Science, Nanjing, China

ARTICLE INFO

Article history:
Available online 11 October 2014

Keywords:
Electron spin resonance dating
Fossil tooth
Quartz grain
Early Pleistocene
Vallparadís
Atapuerca Gran Dolina

ABSTRACT

ESR dating was applied to fossil teeth and optically bleached quartz grain samples from two units of the sequence at Vallparadís (Barcelona, Spain): weighted mean ESR age estimates of 858 ± 87 ka and 849 ± 48 ka were obtained for EVT-7, which includes the archaeological level 10, and EVT-8, respectively. These results are in good agreement with the existing magneto-biostratigraphic framework that constrain these deposits between 780 and 990 ka, and indicate that Vallparadís EVT-7 has a chronology very close to that of Atapuerca Gran Dolina TD-6 (Spain).

1. Introduction

Dating Early Pleistocene archaeological sites in the Mediterranean region is a challenge because most of these sites are found outside of volcanic context, precluding thus the use of the Ar–Ar method. Recent methodological advances have highlighted the potential of other chronometric methods for this time range, such as burial dating based on Al–Be cosmogenic nuclides measured in quartz grains, U–Pb dating of flowstones in cave, or extended-range luminescence dating of quartz and feldspars (e.g. Rhodes et al., 2006; Carbonell et al., 2008; Pickering et al., 2013; Arnold et al., 2015). However, the use of each method is limited by a range of factors (e.g. sedimentary context, depth, presence of carbonates or quartz), which make impossible their application on a systematic basis for every site. In that regard, electron spin resonance (ESR) dating offers an interesting opportunity, since this is a versatile method that may be applied to a wide range of materials such as optically bleached quartz grains, carbonates and fossil teeth, covering thus almost all possible geological contexts for this time range. This is why ESR is the most frequently used method to date early hominin occupations in Europe (see overviews in Falguères, 2003; Bahain et al., 2007; Duval et al., 2012).

However, despite encouraging dating results, ESR has also some limitations that are specific to this time range, which may either preclude any age calculation or generate strong age underestimation (e.g. Duval et al., 2012 for an overview). In particular, the precision that can be obtained in ESR dating may sometimes not be good enough to solve hot debates about the chronology of the first hominin settlements in Europe (Muttoni et al., 2013; Toro-Moyano et al., 2013). Classically, these methodological issues may be addressed by specifically working on sites with good independent age controls, but these are not common in this time range. In that regard, the Vallparadís site represents an excellent case study. A combination of magneto- and bio-stratigraphic studies, together with ESR age estimates obtained on both quartz grains and fossil teeth have helped to constrain the chronology of the main archaeological level around 0.8 Ma ((Madurell-Malapeira et al., 2010; Martínez et al., 2010; Duval et al., 2011a).

In order to complement these promising ESR dating results, additional tooth samples were collected for dating and quartz samples were re-analyzed following recent methodological developments (Duval, 2012; Duval and Guilarte Moreno, 2012). This

* Corresponding author.
E-mail address: mathieu.duval@cenieh.es (M. Duval).

http://dx.doi.org/10.1016/j.quaint.2014.08.054
1040-6182/

work presents an updated synthesis of the ESR age results obtained at Vallparadís.

2. Vallparadís: chronostratigraphic framework and previous ESR dating results

Excavated between 2005 and 2008, the site of Vallparadís is located within the city of Terrassa (Barcelona, Eastern Spain, Fig. 1) and has yielded a ~15 m thick sedimentary sequence made by a succession of fluvial and alluvial sediments associated to the Vallparadís stream. The sequence has been divided into 12 units from the top to the bottom and includes an erosional surface (unit 5) that separates the deposits into two parts (Fig. 2). Several archaeological and paleontological levels have been identified in the sequence, but the excavation has been mainly focused on the richest ones in terms of faunal remains and lithic artifacts, the archaeological levels 10 and 10c, located within stratigraphic unit EVT-7. The whole surface of this unit was excavated, which corresponded to an area of 780 m^2 and an average depth of 1.5–2 m. This excavation yielded a rich bipolar on an anvil Mode 1 lithic assemblage associated to numerous macro- and medium-sized faunal fossil remains, several of which demonstrating hominin access to the herbivore carcasses, such as cut marks and bone fracturing (Madurell-Malapeira et al., 2010; Martínez et al., 2010, 2013, 2014; Garcia et al., 2012, 2013a, 2014).

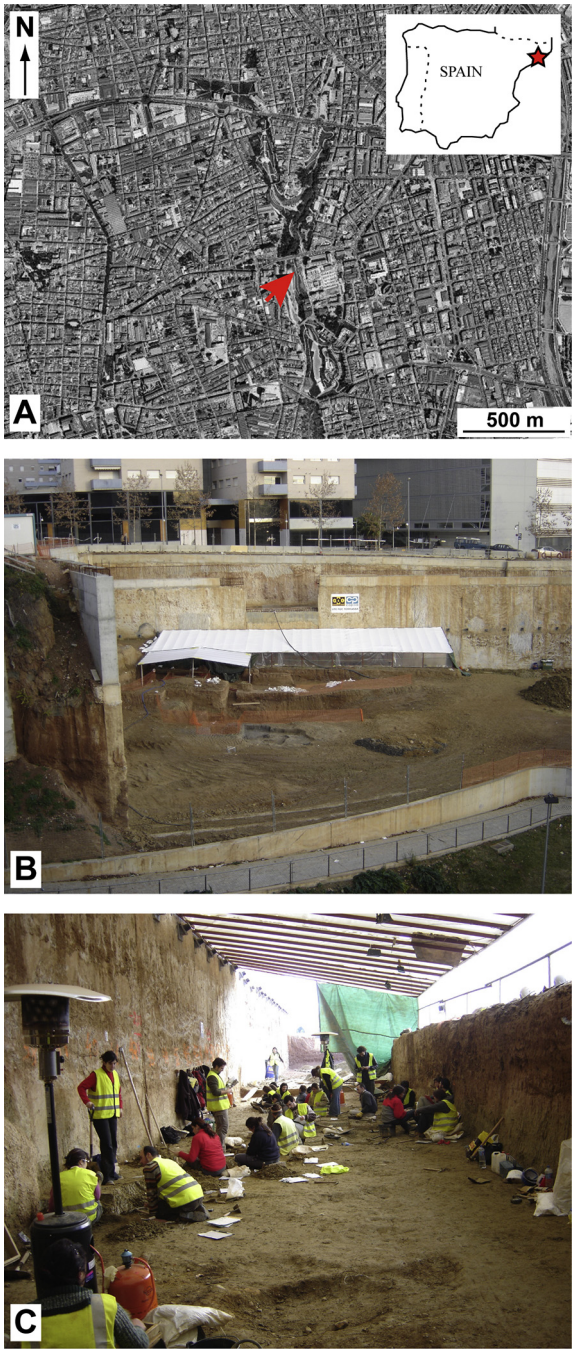

Fig. 1. Vallparadís site. A: Geographical location within the city of Terrassa (Barcelona, Spain). B and C: excavation area.

The chronology of the sequence has been constrained by a combination of magneto- and bio-stratigraphy and ESR dating. Palaeomagnetic studies indicated the record of three magnetozones (Madurell-Malapeira et al., 2010; Martínez et al., 2010): a normal magnetozone N1 at the bottom (unit EVT-12 to mid-unit EVT-8) and another normal N2 at the top of the sequence (from the lower part of unit EVT-3 to the top of unit EVT-2) surrounding a reverse magnetozone R1 (from mid-unit EVT-8 to the bottom of unit EVT-3) that encloses the archaeological levels 10 and 10c. This level yielded a faunal association (Madurell-Malapeira et al., 2010; Martínez et al., 2010), made by a combination of Villafranchian large mammal taxa (e.g. *Pachycrocuta brevirostris*, *Panthera gombaszoegensis*, *Stephanorhinus hundsheimensis*, *Hippopotamus antiquus* and *Pseudodama vallonnetensis*) with a few Galerian species (*Canis mosbachensis*, *Elephas antiquus*, *Ursus deningeri* and *Sus* sp.), that may be attributed to the Epivillafranchian biochron (Madurell-Malapeira et al., 2010; Martínez et al., 2010). This biochron, also named Early Galerian or Protogalerian (Palombo, 2007; Rook and Martínez-Navarro, 2010), corresponds to a period of important faunal renewal in Europe that occurs during the so-called "Early–Middle Pleistocene transition" (Head and Gibbard, 2005) and is usually correlated to a time range spanning from the Jaramillo subchron to the late part of the Early Pleistocene (Kahlke, 2009; Rook and Martínez-Navarro, 2010). The micromammal assemblage found in level 10 (EVT-7) of Vallparadís is made up of the following species: *Ungaromys nanus*, *Iberomys huescarensis*, *Mimomys savini*, *Eliomys quercinus*, *Apodemus* sp., *Talpa europaea*, *Crocidura* sp., *Stenocranius gregaloides*, *Apodemus* cf. *sylvaticus* and *Hystrix refossa* (Minwer-Barakat et al., 2011; Martínez et al., 2010, 2014). This association may be correlated with the *Allophaiomys chalinei* (recently redefined as *Victoriamys chalinei* by Martin, 2012) biozone defined by Cuenca-Bescós et al. (2010) at Atapuerca Gran Dolina for levels TD3 to TD8a, and ranging in age from the end of the Early Pleistocene (>0.78 Ma) to the beginning of the Middle Pleistocene (around 600 ka) (Falguères et al., 1999; Parés and Pérez-González, 1999; Duval et al., 2012). According to Minwer-Barakat et al. (2011), the absence of *V. chalinei* in EVT-7 should not be interpreted as a biochronologic indication, but is probably due to the scarcity of the rodent material that has been found at Vallparadís.

Preliminary ESR dating of optically bleached sedimentary quartz grains and combined U-series/ESR dating of fossil teeth samples provided an initial ESR chronology of ~0.8 Ma for Vallparadís: 0.79 ± 0.23 Ma (2σ) for unit EVT-12 and 0.83 ± 0.13 Ma (2σ) for unit EVT-7 (Martínez et al., 2010; Duval et al., 2011a). These results are in good agreement with the magnetostratigraphy, indicating that N1 and N2 could be correlated to Jaramillo and Brunhes, constraining thus unit EVT-7 between 0.99 and 0.78 Ma (Martínez et al., 2010, 2014; Duval et al., 2011a).

In detail, two horse fossil teeth (EVT0601 and EVT0602) from unit EVT-7 were analyzed but only the first one provided a combined US-ESR age. Sample EVT0602 showed extremely high $^{230}Th/^{234}U$ ratios in the three dental tissues with apparent age

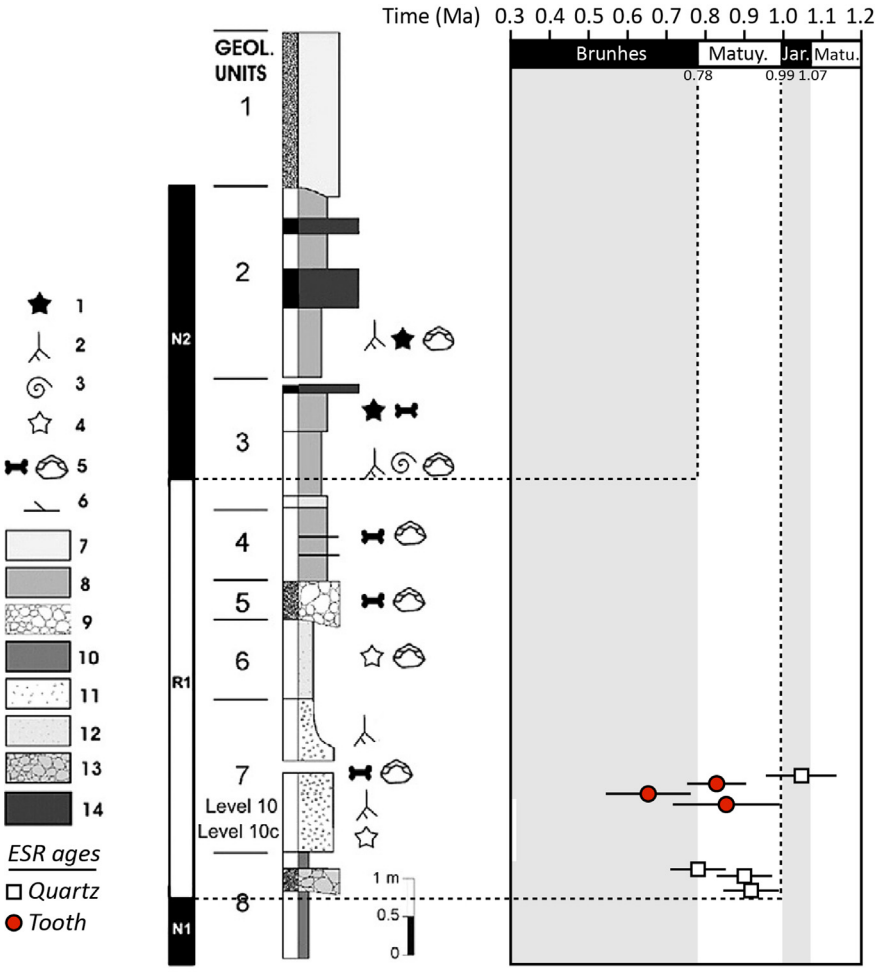

Fig. 2. Chronostratigraphy of the sedimentary sequence at Vallparadís (modified from García et al., 2013a), including palaeomagnetic data and new ESR ages (1σ) obtained on fossil teeth and quartz grains. Key: (1) organic material and fossil wood remains, (2) root marks, (3) gastropod remains, (4) $CaCO_3$ remains, (5) units bearing archaeological remains, (6) cross-lamination, (7) Upper Pleistocene terrace, (8) clays and muds with gastropods, (9) unit 5, (10) red clays and muds, (11) unit 7 (levels 10 and 10c), (12) brown clays and muds, (13) conglomerates, and (14) paleo-floor.

>280 ka (Duval et al., 2012) that precluded any combined US-ESR age calculation, while sample EVT0601 provided an age estimate of 0.83 ± 0.07 Ma (Martínez et al., 2010). To complement these first results, two additional equid teeth (EVT1001 and EVT1002) were collected from the same archaeological layer 10 (geological unit EVT-7) and were dated with the combined US-ESR approach (Grün et al., 1988).

Initial ESR results obtained on quartz grains showed consistent age estimates around ~0.8 Ma (Duval et al., 2011a). However, the magnitude of the relative error was especially high (between 20 and 33% at 1σ). This large uncertainty mainly originates from the ESR dose estimation, particularly in the fitting of the dose response curve (DRC). This is why these four samples were re-analysed following the recommendations by Duval (2012) to ensure a reliable and good fitting in terms of number of dose steps, choice of the maximum irradiation dose and goodness-of fit, and measured at low temperature under controlled and stable experimental conditions (Duval and Guilarte Moreno, 2012).

3. Material and method

3.1. ESR dating of fossil teeth

EVT1001 and EVT1002 were prepared in the same way as the previous ones (Martínez et al., 2010). The sampling area was focused on the vestibular side of the teeth, and the three dental tissues (cement, enamel, and dentine) were separated mechanically. The enamel layer was cleaned on both sides (inner and outer) to eliminate the effect of external alpha contribution, then was ground and sieved. Equivalent dose (D_E) measurements were performed on the 100–200 μm enamel powder using a multiple-aliquot additive-dose (MAA) protocol involving irradiation steps up to 60 kGy with a calibrated γ source.

ESR measurements were carried out at room temperature with the following acquisition parameters: 1 mW microwave power, 1024 points resolution, 100 kHz modulation frequency, 0.1 mT modulation amplitude, 20 ms conversion time, and 5 ms time constant. Each aliquot set was measured several times at different days to check reproducibility. The ESR intensities were extracted from peak-to-peak amplitudes (T1-B2) of the ESR signal of enamel (Grün, 1998). The D_E values and associated errors were obtained by fitting procedures carried out with the Microcal OriginPro 8.5 software using a Levenberg–Marquardt algorithm by chi-square minimization. Data were weighted by the inverse of the squared ESR intensity (Grün and Brumby, 1994). A double saturating exponential (DSE) fitting function, made by the combination of two exponential terms, was used (see further details in Duval et al., 2013). An example of dose response curve (DRC) is shown in Fig. 3.

U-series analyses of each dental tissue were performed by ICP-QMS, according to the standard procedure described in Shao

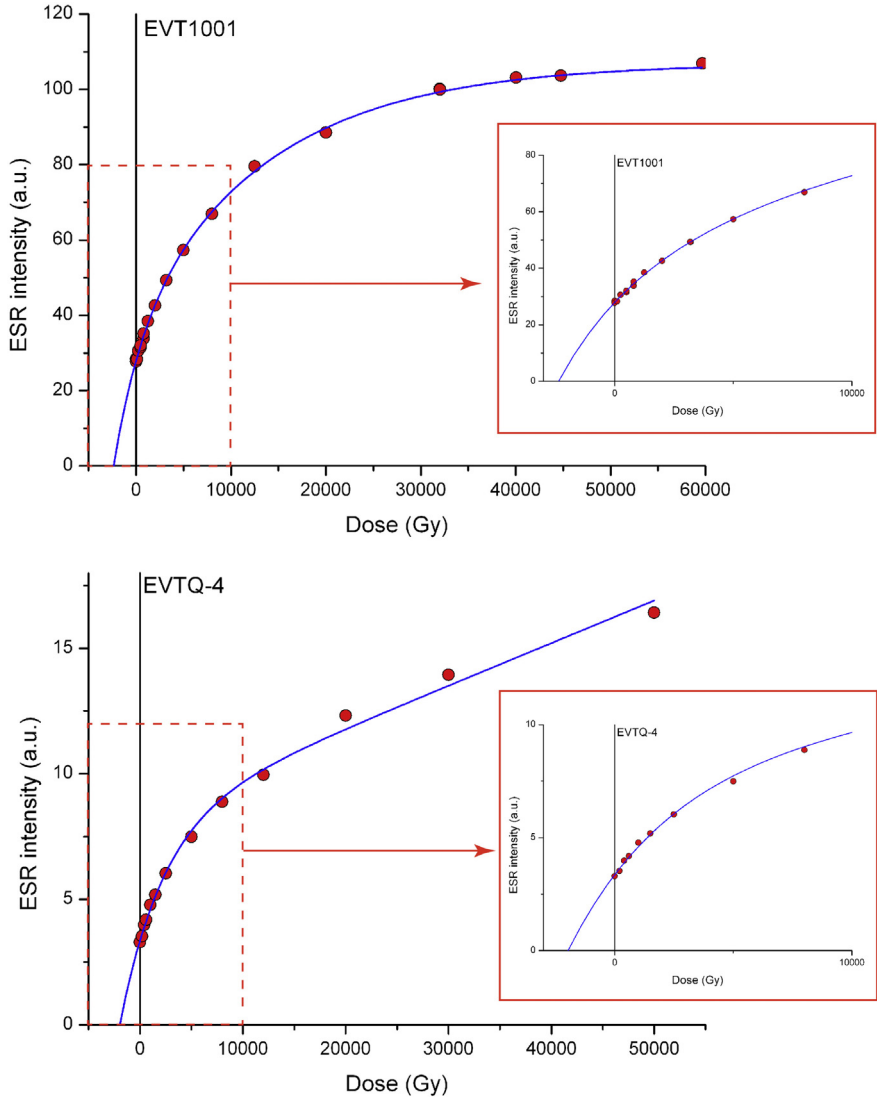

Fig. 3. Examples of ESR dose response curves obtained from a fossil tooth (top) and a quartz (bottom) sample from Vallparadís.

(2011). Combined US-ESR age calculations based on Grün et al. (1988) were carried out with the USESR program (Shao, 2011) using an alpha efficiency of 0.13 ± 0.02 (Grün and Katzenberger-Apel, 1994) and Monte-Carlo beta attenuation factors from Brennan et al. (1997) based on the thickness of the tooth enamel and outer layers removed. The water content was estimated to be 3 ± 1 wt% in the enamel, 5 ± 3 wt% in the dentine and cement, and 15 ± 5 wt% in the sediment, the latter one based on the dried weight. The effect of Ra and Rn loss in each tissue was determined by combining alpha-ray and gamma-ray data (Bahain et al., 1992). Gamma-ray spectrometry was used to determine the radioisotope (U, Th, and K) contents of sediments which were taken *in situ* (Yokoyama and Nguyen, 1980). *In situ* gamma dose rate was assessed by placing two TL dosimeters (CaSO4:Dy) in Unit EVT-7 (level 10) for 10 months. Cosmic component was calculated from Prescott and Hutton (1994). Final age errors were assessed by Monte Carlo simulations and are given at 1σ (Shao, 2011).

Additional U-series analyses of a cross section of sample EVT1001 were performed by laser ablation multi-collector ICP-MS at RSES (Canberra, Australia), using a custom-built laser sampling system interfaced between an ArF Excimer laser and a Finnigan Neptune (for details, see Eggins et al., 2003, 2005). Data reduction followed Grün et al. (in press) using the dentine of a rhinoceros tooth from Hexian (sample 1118, see Grün et al., 1998) as a secondary matrix matched standard.

3.2. ESR dating of optically bleached quartz grains

A new ESR dosimetry study was performed on the four sediment samples (EVTQ-1, EVTQ-2, EVTQ-3 and EVTQ-4) that were collected in 2006. Details about sample preparation may be found in Duval et al. (2011a). Quartz grains of the 100–200 μm fraction were divided into 13 aliquots and irradiated with a calibrated Gammacell-1000 Cs-137 gamma source up to 50 kGy. ESR measurements were performed at low temperature (~90 K) using a ER4141VT Digital Temperature control system based on liquid nitrogen cooling (see Duval and Guilarte Moreno (2012) for further details about the experimental setup and about its stability over time), using the following acquisition parameters for the analysis of the Aluminum (Al) center: 10 mW microwave power, 1024 points resolution, 20 mT sweep width, 100 kHz modulation frequency, 0.1 mT modulation amplitude, 40 ms conversion time, 10 ms time constant and 1 scan. Each aliquot was measured 3 times after a ~120° rotation in the cavity. This procedure was repeated over three

Table 1
U-series data obtained for each dental tissue of the two tooth samples. Key: E = enamel, D = dentine and C = cement.

Sample	Tissue	U (ppm)	$^{234}U/^{238}U$	$^{230}Th/^{234}U$	$^{222}Rn/^{230}Th$	$^{230}Th/^{234}U$ age (ka)
EVT1001	E	2.853 ± 0.010	1.949 ± 0.003	0.975 ± 0.008	1.00 ± 0.01	220
	D	101.2 ± 0.681	2.157 ± 0.004	1.056 ± 0.054	1.00 ± 0.01	266
	C	66.45 ± 0.643	2.079 ± 0.004	1.063 ± 0.020	0.39 ± 0.05	275
EVT1002	E	1.397 ± 0.004	1.784 ± 0.007	0.905 ± 0.008	1.00 ± 0.01	188
	D	85.95 ± 0.682	2.146 ± 0.003	1.083 ± 0.012	0.34 ± 0.10	290

to four different days without removing the quartz samples from the ESR tubes between measurements. The non-bleachable residual ESR signals of the Aluminium center were obtained after exposing an aliquot of each natural sample in a SOL2 (Dr Hönle) solar light simulator for ~1460 h (Duval et al., 2011a). The ESR intensity of the Al signal was extracted from peak-to-peak amplitude measurements between the top of the first peak (g = 2.0185) and the bottom of the 16th peak (g = 1.9928) (Toyoda and Falguères, 2003).

The equivalent dose (D_E) and associated error were obtained by fitting procedures carried out with the Microcal OriginPro 8.5 software, with ESR data weighted by the inverse of the squared ESR intensity ($1/I^2$). A function combining an exponential and linear terms (EXP + LIN) was used (see equations in Duval, 2012). D_E values were obtained by extrapolating the EXP + LIN function to the residual (= non-bleachable ESR signal) level. An example of dose response curve (DRC) is shown in Fig. 3.

ESR age calculations were performed using the following parameters: alpha attenuation from Brennan et al. (1991) and beta attenuation values for spherical grains from Brennan (2003) assuming an average initial grain size of 150 μm and 20 μm of etching, water content correction from Grün (1994) and dose rate conversion factors from Guérin et al. (2011). Water content was assumed to be 15 ± 5%. Cosmic dose rate was calculated from Prescott and Hutton (1994), including latitude, depth and altitude corrections. An internal dose of 50 ± 30 μGy/a was considered, based on the average U and Th concentrations of 0.08 ± 0.02 and 0.18 ± 0.03 ppm measured by Vandenberghe et al. (2008) in purified quartz samples and assuming an alpha efficiency *k* of 0.15 ± 0.10 (Yokoyama et al., 1985). ESR age calculations were performed using a non-commercial SCILAB based software, with error calculations derived from Monte Carlo simulations. ESR ages are given at 1σ.

4. Results and discussion

4.1. Combined US-ESR dating of fossil teeth

U-series and US-ESR data obtained for samples EVT1001 and EVT1002 are shown in Tables 1 and 2. These two teeth show a similar isotopic signature to that of the two previously published teeth, with high $^{234}U/^{238}U$ value (up to 2.157) and $^{230}Th/^{234}U$ ages overall >200 ka (Duval et al., 2012). Combined US-ESR dating performed on these samples yield consistent age estimates at 1 σ of 662 ± 111 and 856 ± 141 ka for EVT1001 and EVT1002, respectively. Nevertheless, one may observe that the age obtained for EVT1002 is in good agreement with the existing chronostratigraphic framework of the site constraining EVT-7 layer between 780 and 990 ka, whereas the age derived from EVT1001 seems somewhat underestimated. To explain this, the hypothesis of some overestimation of the gamma dose rate due to lateral variation of *in situ* dosimetry can be discarded, given that the two TL dosimeters that have been left a few meters apart in level 10 registered almost the same values (971 ± 54 μGy/a and 973 ± 47 μGy/a).

Fig. 4 is a plot of the values obtained for each component of the dose rate of the two samples, including also the data from sample EVT0601 analysed in previous works (Martínez et al., 2010; Duval et al., 2011a). This graph shows that the dose rate value for sample EVT1001 (4394 ± 1042 μGy/a) is significantly higher than those calculated for EVT0601 and EVT1002 (2944 ± 244 and 2563 ± 518 μGy/a, respectively), which explain the younger age obtained for this sample. Such a difference is mainly coming from the dental tissues, in particular the internal

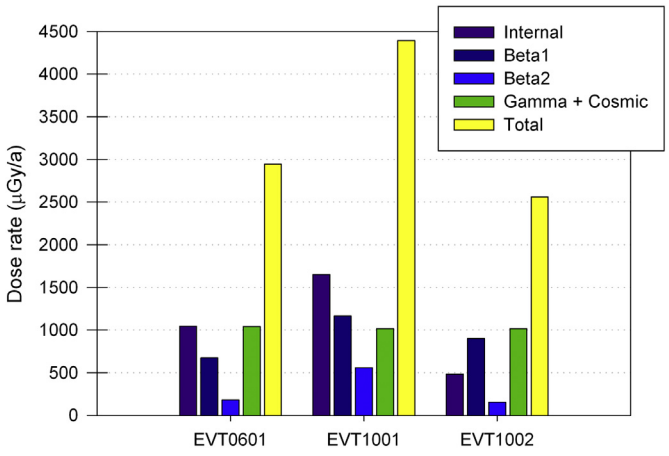

Fig. 4. Values obtained for the various components of the dose rate for the teeth EVT0601, EVT1001 and EVT1002. Samples EVT1001 and EVT1002 were analysed in the present study, whereas data for sample EVT0601 are taken from Martínez et al. (2010) and Duval et al. (2011a). Combined US-ESR age calculation was impossible for the tooth sample EVT0602. Key: the internal dose rate is for enamel, and is made by an alpha and a beta dose rate contribution; Beta1 is the beta dose rate contribution from the inner side (i.e., dentine) of the enamel layer, while Beta2 is the beta dose rate contribution from the outer side (i.e., cement for samples EVT0601 and EVT1001 and sediment for EVT1002) of the enamel layer; Gamma + Cosmic correspond the gamma dose rate from the sediment plus the contribution from the cosmic rays.

Table 2
Combined US-ESR age results obtained for samples EVT1001 and EVT1002. Key: E = enamel, D = dentine and C = cement.

Sample	Unit (layer)	Depth (m)	α + β internal (μGy/a)	β dentine (μGy/a)	β cement (μGy/a)	γ sediments + cosmic (μGy/a)	Total dose rate (μGy/a)	*p*-values			D_E value (Gy)	Age (ka)
								Enamel	Dentine	Cement		
EVT1001	7 (10)	9 ± 2	1650 ± 819	1165 ± 578	560 ± 278	1018 ± 57	4394 ± 1042	−0.52	−0.71	−0.75	2909 ± 488	662 ± 111
EVT1002	7 (10)	9 ± 2	486 ± 243	902 ± 454	155 ± 18	1018 ± 57	2563 ± 518	0.02	−0.86	–	2194 ± 257	856 ± 141

dose rate of the enamel and the beta dose rate from the cement. Dental tissues represent between 54% (EVT1002) and 77% (EVT1001) of the total dose rate. This is actually one of the main specificities of Early Pleistocene samples, compared to younger ones: because these "old" samples show high U-concentrations (>100 ppm sometimes in dentine), the U-uptake that is modeled has a major impact on the final age estimate (Grün and McDermott, 1994; Duval et al., 2012). In the combined US-ESR approach, the U-uptake history is directly derived from the U-series data measured for each dental tissue. Therefore, the reliability of the calculated US-ESR age directly depends on the accuracy of these U-series data.

To get further insights about the spatial distribution of U-series data in dental tissues, one LA-ICP-MS profile was performed on a transversal section of EVT1001, across cement, enamel and dentine (Fig. 5). The cross section was cut in the lower half part of the tooth, while bulk U-series and ESR analyses were done in the upper half of the tooth. The difference in sampling location within the tooth sample may explain why LA-ICP-MS and bulk U-series data set do not necessarily match, given the spatial variations (horizontally and vertically) that have been previously observed in Early Pleistocene fossil teeth (Duval et al., 2011b). Numerical values from the LA track were extracted in Table 3. Each tissue shows a distinct pattern. U-series values remain overall constant across dentine. In contrast,

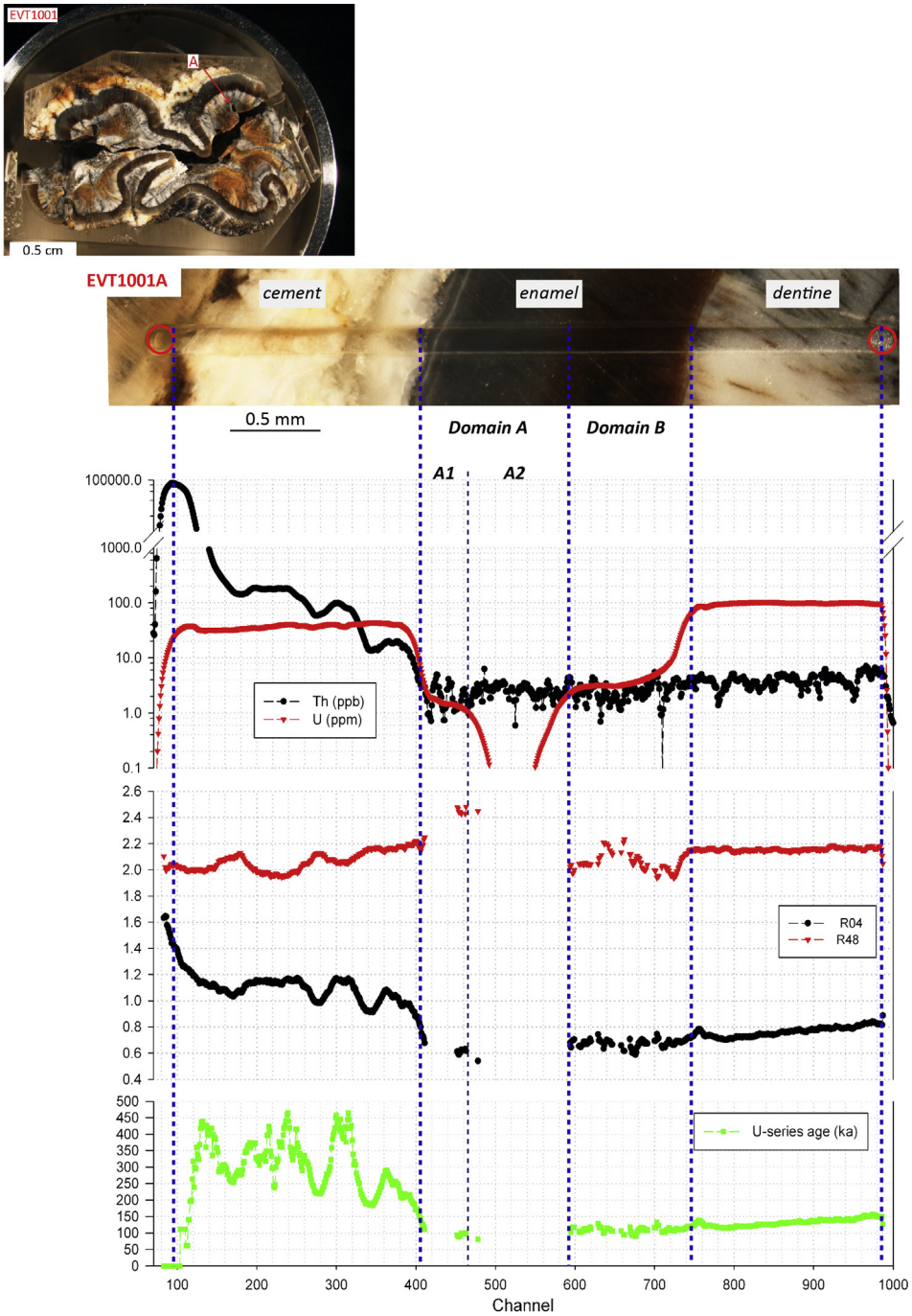

Fig. 5. : LA-ICP-MS U-series ablation profile across EVT1001 showing the following data: ^{232}Th and ^{238}U concentrations (top), ^{234}U/^{238}U (labelled R48 in the figure) and ^{230}Th/^{234}U ((= R04) in the figure) activity ratios (middle) and U-series age (bottom graph).

Table 3
U-series data extracted from laser ablation track A performed on EVT1001. Key: s.d. = standard deviation; c.v. = coefficient of variation (i.e. relative standard deviation).

Domain	Channel range	^{232}Th (ppb)			^{238}U (ppm)			^{230}Th/^{234}U			^{234}U/^{238}U			^{230}Th/^{234}U age (ka)		
		Mean	s.d.	c.v.	Mean	s.d.	c.v.	Mean	s.d.	c.v.	Mean	s.d.	c.v.	Mean	s.d.	c.v.
Cement	100–380	5107.6	16,564.4	324%	37.9	3.8	10%	1.10	0.08	8%	2.06	0.07	3%	300.2	92.4	31%
Enamel-A	440–580	2.4	0.8	32%	0.5	0.5	110%	0.60	0.03	5%	2.45	0.02	1%	93.1	6.7	7%
Enamel-B	600–720	2.4	0.9	40%	3.9	1.2	30%	0.67	0.03	5%	2.06	0.06	3%	109.1	8.9	8%
Dentine	760–980	3.9	1.0	26%	100.2	4.0	4%	0.76	0.04	5%	2.16	0.01	0%	131.6	10.6	8%

the cement shows more important lateral variation, with a gradient from the external side towards the Cement–Enamel Junction (CEJ): ^{232}Th concentration is very high in the edge of the cement, in contact with the sediment, and then decreases towards the interior, while ^{234}U/^{238}U and ^{230}Th/^{234}U ratios show opposite trends. The first increases towards the interior (from ~2.0 to ~2.2), whereas the second decreases (from ~1.6 to ~0.8). This may indicate a change in the hydrological conditions over time. If U-series data derived from bulk U-series analysis (Table 1) and mean values from LA-ICP-MS analysis (Table 3) show somewhat consistent ^{234}U/^{238}U and ^{230}Th/^{234}U ratios, the spatially resolved data provide nevertheless crucial additional information about the migration of U-series elements into cement that could simply not be observed with a single bulk analysis. The apparent U-series ages are not constant along the ablation profile and data are obviously influenced by the presence of detrital ^{232}Th in cement. The outer part of the cement (channels 80–100) shows a decrease of the U-concentration, associated with an increase of the ^{230}Th/^{234}U ratio, indicating thus U-leaching process at the edge of the cement. Given these observations, one may reasonable question the meaning of the apparent U-series ages obtained for cement and their impact on combined US-ESR dating. As with dentine or bone, cement is known to be more sensitive to diagenetic alteration than dental enamel. Its position protecting one side of the enamel layer and in direct contact with the sediment make it very likely the first tissue affected by weathering processes.

Finally, the enamel layer can be clearly divided in two different domains: the left domain (domain A) is mainly grayish while the right part, on the dentine side, has a brownish color. These two domains show two distinct U-series patterns. Overall, domain A shows highly varying U-concentration values that are on average about 0.5 ± 0.5 ppm. Most are below the detection limit of the LA-ICP-MS for these acquisition parameters, yielding very scattered data that have been removed from the graph for a sake of clarity. Domain A may be divided into two sub-domains, A1 and A2. A1 is the front of uranium uptake coming from the cement, with especially high ^{234}U/^{238}U values and quite recent apparent U-series age. In contrast, domain A2 shows virtually no uranium, the concentrations drop below 0.1 ppm. This domain is potentially of special interest for ESR dating, since in that specific area the internal dose would be very low, and any U-uptake assumption would have a negligible impact on the final age. Domain B may be interpreted as the U-uptake front from the dentine, with a mean U-concentration of 3.9 ± 1.2 ppm and a depth into enamel >2 times higher than that of the cement (0.60 vs 0.25 mm respectively). This indicates that uranium uptake is mainly coming from the dentine side, which is in agreement with previous observations (e.g. Duval et al., 2011b). In contrast with domain A2, a specific micro sampling of enamel within domain B would yield a massive internal dose rate, which is known to be a major source of uncertainty in ESR dating (e.g. Duval et al., 2012). However, the direct impact on the final ESR age is for the moment hardly quantifiable since many parameters are involved in the calculation process. These results indicate nevertheless that new sampling strategies should be developed in the future to collect several powder micro-samples from various domains of the enamel layer of a given sample showing different U-series features, in order to accurately assess the real impact of these observations on the final age result (Grün and Duval, 2014).

4.2. ESR dating of quartz grains

New gamma irradiations (13 dose steps up to 50 kGy, compared to 11 dose steps up to 25 kGy in the previous study by Duval et al., 2011a) and ESR measurements performed on the quartz samples provided D_E results ranging from 2077 ± 225 to 2576 ± 371 Gy. These new fitting results all show $r^2 > 0.99$ and relative D_E errors <15%, ensuring thus a reliable fitting (see Duval et al., 2013). Table 4 shows a comparison between these new results and those previously published by Duval et al. (2011a) using the same EXP + LIN function: D_E results are consistent at 1 sigma for 3 of the samples, the exception being EVTQ-4. However, in Duval et al. (2011a) samples EVTQ-2, EVTQ-3 and EVTQ-4 show a regular goodness-of-fit ($r^2 < 0.99$), with very high relative D_E error (between 20.3 and 33.1%) in comparison with the present study. The only exception is sample EVTQ-1, with similar goodness-of-fit and D_E values. The improved accuracy of these new ESR data may be very likely the result of a combination of several factors, such as a higher number of irradiated aliquots measured for the DRC (13 vs 11 previously) and the excellent stability of the experimental setup at CENIEH, allowing highly repeatable ESR measurements (Duval and Guilarte Moreno, 2012).

ESR age estimates were calculated using a combination of EXP + LIN functions as described in Duval (2012) and assuming equilibrium in the U-series. Results are shown in Table 5. The ages obtained for the four quartz samples clearly indicate an Early Pleistocene chronology, ranging from 778 ± 72 ka (EVTQ-0601) to 1046 ± 89 ka (EVTQ-0604). They are all consistent at 1 sigma with the previous ESR ages published by Duval et al. (2011a). Nevertheless, the errors on the ESR age estimates are significantly smaller and range from 6% to 8% (1 σ), vs 20%–33% previously. This is mainly due to a better precision in the D_E values.

Table 4
Comparison of the new fitting results obtained for the 4 quartz samples with those previously published by Duval et al. (2011a), using the following EXP + LIN function (Duval, 2012): $I(D) = I_{sat}{}^{*}(1-\exp[-(D+ D_E)/D_0] + m^{*}D$. For a matter of consistency, the latter were obtained by running a new fitting with OriginPro 8.5 through the original ESR data set, which may explain some slight differences (<1%) with the D_E values originally published by Duval et al. (2011a) and obtained with Origin 6.5.

	Duval et al. (2011a)			This work		
	D_E (Gy)	Rel. Error (%)	Adj. r^2	D_E (Gy)	Rel. Error (%)	Adj. r^2
EVTQ-1	1891 ± 201	10.6%	0.997	2077 ± 225	10.8%	0.995
EVTQ-2	2049 ± 416	20.3%	0.989	2576 ± 371	14.4%	0.992
EVTQ-3	2155 ± 713	33.1%	0.979	2549 ± 299	11.7%	0.994
EVTQ-4	1280 ± 362	28.3%	0.978	2133 ± 239	11.2%	0.995

Table 5
ESR dating results obtained for the 4 quartz samples. Age calculation was performed for each sample using a mean D_E value derived from two EXP + LIN functions with different linear terms (for further details and function equations, see Duval, 2012).

Sample	EVTQ-1	EVTQ-2	EVTQ-3	EVTQ-4
Unit (layer)	8(12)	8(12)	8(12)	7 (10)
Depth (m)	11 ± 2	11 ± 2	11 ± 2	9 ± 2
Internal dose rate (μGy/a)	50 ± 30	50 ± 30	50 ± 30	50 + 30
Alpha dose rate (μGy/a)	40 ± 34	44 ± 37	44 ± 37	23 + 20
Beta dose rate (μGy/a)	1535 ± 118	1583 ± 118	1612 ± 122	866 ± 65
Gamma dose rate (μGy/a)	918 ± 77	1030 ± 85	957 ± 80	971 ± 83
Cosmic dose rate (μGy/a)	46 ± 10	46 ± 10	46 ± 10	58 ± 14
Total dose rate (μGy/a)	2592 ± 192	2756 ± 201	2712 ± 198	1972 ± 144
D_E (Gy)	2005 ± 107	2479 ± 168	2464 ± 159	2051 ± 85
Age (ka)	778 ± 72	905 ± 91	914 ± 90	1046 ± 89

The three samples located within the top of unit 8 (EVTQ-1, EVTQ-2 and EVTQ-3) yield ESR ages ranging from 778 ± 72 ka to 914 + 90 ka (Fig. 4). The younger ESR age estimate obtained for EVTQ-1 is mainly due to the D_E value (Table 5), which is somewhat lower than those calculated for the two other samples, while the total dose rate values vary within narrow range (2592 ± 192 to 2756 ± 201 μGy/a). Nevertheless, the ESR results obtained for the 3 samples are not significantly different, since they are all consistent at 1 sigma: a weighted mean age of 849 ± 48 ka (1 σ) may be thus calculated for unit EVT8 of Vallparadís. A slight U-series disequilibrium (Rn-loss) has been observed in some of the sediment samples. Dose rate calculation performed considering pre-Rn dose rate conversion factors induce a slight decrease of the dose rate, making thus the age older by 2–3%. The weighted mean age derived from this option is of 871 ± 48 ka, i.e. very close to the results derived from equilibrium. However, we do not have any evidence showing these U-series disequilibrium conditions have prevailed over the burial history of the sample. Consequently, we consider the conservative option assuming U-series equilibrium should be used as a reference for unit EVT-8 of Vallparadís. This new mean age is in good agreement with the previous age of 787 ± 118 ka (1σ) obtained by Duval et al. (2011a), but with a much better precision.

The sample EVTQ-4 from Unit 7 (layer 10), about 2 m above the other samples, provides an age of 1046 ± 89 ka that is apparently overestimated in comparison with the other ages based on quartz grains. Nevertheless, this ESR age estimate should not be considered as inconsistent since this is not in disagreement with the other ages at 2 σ. Such age overestimation might be linked to the beta dose rate, which is about 2 times lower than the beta dose rate values calculated for the other samples. Unit EVT-7 is made by heterogeneous coarse deposits in a sandy matrix (Martínez et al., 2010, 2013; Garcia et al., 2012), which may cause some important local variations in the beta microdosimetry.

4.3. Biochronological implications

Three combined US-ESR ages on fossil teeth and one ESR age on quartz are available for level 10: 830 ± 70 ka (EVT0601), 662 ± 111 ka (EVT1001), 856 ± 141 ka (EVT1002) and 1046 ± 89 ka (EVTQ-4) (Fig. 2). Age scatter is somewhat important, but ESR age estimates are nevertheless all consistent at 2 sigma, given the magnitude of the uncertainties of each individual date. Consequently, there is no apparent reason to consider any of these data as outlier: the weighted mean age of the four data is 858 ± 87 ka (1σ). This age is statistically indistinguishable from the age obtained for the unit 8 located below 849 ± 48 ka (1σ). These ESR results place Vallparadís in the latest part of the Early Pleistocene, similarly to Dolina TD-6 (Atapuerca), whose ESR chronology based on fossil teeth has been recently updated to 766 ± 81 ka (Duval et al., 2012). Recent palaeomagnetic data indicate the presence of short normal magnetozones within TD7 that might be correlated to Kamikatsura and/or Santa Rosa subchrons, suggesting thus a chronology older than 936 ka for TD-6 (Parés et al., 2013a). However, recent single-grain TT-OSL age estimates based on quartz grains from TD-6 yielded a weighted mean age of 846 ± 57 ka (Arnold et al., 2015), which is more consistent with the existing ESR chronology (Falguères et al., 1999; Duval et al., 2012). Consequently, if Vallparadís appears to be slightly older than Gran Dolina TD-6 from the ESR dating point of view, the overlapping age errors do nevertheless not allow these sites to be differentiated, and they should thus be considered as coeval.

Looking at large mammal biochronology, this new ESR chronology may contribute to refine the time range covered by the Epivillafranchian biochron. The Colle Curti Colle faunal unit (FU) is usually taken as one of the references (together with the locality of Untermassfeld, Kahlke, 2009) for the Early Galerian (= Epivillafranchian) and has a chronology that has been correlated to the Jaramillo subchron (1.07–0.99 Ma) (e.g. Coltorti et al., 1998; Masini and Sala, 2007; Palombo, 2007). However, as highlighted by Madurell-Malapeira et al. (2010), the large mammal record at Vallparadís significantly extends the time range covered many Villafranchian carnivore taxa (e.g. *P. brevirostris*, *Lycaon lycaonoides*, *P. gombaszoegensis* and *Puma pardoides*) to the latest part of the Early Pleistocene. Consequently, Vallparadís EVT-7 may be considered as one of the youngest evidence of Epivillafranchian assemblage in Europe, indicating that this faunal complex may persist in the Iberian Peninsula perhaps a bit longer than suggested by Kahlke (2009), i.e. up to 800–900 ka. This might however raise some questions about the chronology that is commonly accepted for the transition between Epvillafranchian/Early Galerian and Middle Galerian biochrons. If Kahlke (2009) estimated the end of the Epvillafranchian around 0.9 Ma, in the Italian large mammal record it is usually considered that the Slivia FU (which defines the earliest part of the Middle Galerian) starts some time before the Brunhes-Matuyama boundary, perhaps even around the MIS25 (Masini and Sala, 2007). However, it seems that most of (if not all) the key Italian localities sites for the Slivia FU (e.g. Riffreddo, Ponte Galeria, Slivia) have actually a post-Matuyama (<0.78 Ma) chronology (e.g. Bon et al., 1992; Gliozzi et al., 1997; Petronio and Sardella, 1999; Masini et al., 2005; Masini and Sala, 2007), while the assumed pre-Brunhes age of this biochron is mainly based on correlation with non-Italian localities (Masini et al., 2005). As already suggested by Rook and Martínez-Navarro (2010), it may be necessary to formalize further definition of the Epivillafranchian biochron, not only in terms of mammal association, but also by refining its chronological position and evaluating the possibility of a diachronic evolution with time throughout the European continent.

In terms of small mammal biochronology, there is a general consensus on attributing EVT-7 to the *V. chalinei* biozone (Minwer-Barakat, 2011). This biozone includes many other Spanish palaeontological sites such as Huescar-1, El Chaparral, Cal Guardiola D5, Almenara-Casablanca 3, Puerto Lobo, Loma Quemada, Gran Dolina TD3-8a (Cuenca-Bescós et al., 2010; Minwer-Barakat et al., 2011; López-García et al., 2012 and references therein). Other sites located outside of Spain are also sometimes mentioned as being part of the same biozone, such as Le Vallonnet (France) and Untermassfeld (Germany) (Minwer-Barakat et al., 2011; Garcia et al., 2013b). However, it seems that these attributions are mainly done on the basis of their supposedly secure Jaramillo chronologies, rather than on similarities in the faunal assemblage since their rodent associations do not include any taxa of the *V. chalinei* biozone as defined by Cuenca-Bescós et al. (2010). In

addition, correlations of rodent assemblage between such distant localities should be considered with caution, as biogeographic provincialism may become a major source of uncertainty for chronological inferences (e.g. Gómez Cano et al., 2011). For example, some authors highlight the discrepancies between the supposed Jaramillo age of Untermassfeld and the biochronological interpretation of the site (Van Kolfshoften and Markova, 2005; Maul and Markova, 2007). From the composition of the rodent assemblage, Van Kolfschoten and Markova (2005) suggest a chronology around the Brunhes-Matuyama Boundary, i.e. significantly younger than previously assumed. The interpretation of palaeomagnetic data at this site have also been recently questioned (Muttoni et al., 2013; Parés et al., 2013b). At Le Vallonnet, the coexistence of *Mimomys* sp. with *Allophaiomys* aff. *nutiensis* with Middle Pleistocene taxa like *Arvicola terrestris cantiana* (Paunescu, 2001; Echassoux, 2004) in the rodent assemblage makes the biochronological interpretation of the site quite complicated. In addition, other taxa such as *I. huescarensis* or *V. chalinei* have not been reported by either Echassoux (2004) or Paunescu (2001). Moreover, palaeomagnetic data obtained at this site are not entirely conclusive (Gagnepain, 1996; Muttoni et al., 2013; Parés et al., 2013b). All together, it seems that there is no apparent reason to correlate these localities to the *V. chalinei* biozone as defined by Cuenca-Bescós et al. (2010).

Consequently, among all these sites belonging to the *V. chalinei* biozone, so far only Vallparadís and Gran Dolina sites have a chronology based on a combination of numerical ages and magnetostratigraphy: they should thus be used as references to assess the time interval covered by this biozone. At Gran Dolina, the *V. chalinei* biozone is spanning from TD3 to TD8a layers (Cuenca-Bescós et al., 2010). No numerical ages are available for TD3, whereas combined US-ESR dating of fossil teeth from TD8 have provided a mean age of 610 ± 65 ka (1σ) for this layer (Falguères et al., 1999; Parés et al., 2013). At Vallparadís, Minwer-Barakat et al. (2011) identified the same rodent assemblage from EVT12 to EVT-7, while unit EVT-3 located more than 3 m above, belongs to another biozone. From a biostratigrahic perspective, the rodent assemblage remains apparently unchanged from Jaramillo to at least 858 ± 87 ka, EVT-7. Consequently, the chronology of the lower boundary of *V. chalinei* biozone may be derived from EVT12 and the upper boundary from the age of TD8: this biozone apparently covers an approximated time range from at least Jaramillo (1.07 Ma) to the early Middle Pleistocene (~610 ka) in the Iberian Peninsula.

To refine the chronology of the sites within this biozone, new approaches have been developed, based on the evaluation of the degree of evolution of rodent teeth. For example, Martínez et al. (2010) suggested an older chronology for EVT-7 in comparison with TD-6, based on the morphology of the molars of *I. huescarensis*. They concluded that the elements from EVT-7 were biochronologically older than at Gran Dolina TD4 and closer to Sima del Elefante TE9, dated to 1.1–1.2 Ma (Carbonell et al., 2008), and Huescár-1. However, such an interpretation is weakened by the results from Cuenca-Bescós et al. (2013) who recently discarded the presence of *I. huescarensis* at Elefante. In addition, a recent multitechnique luminescence dating study (single-grain OSL, single-grain TT-OSL, post IR-IRSL) at Huescár-1 yielded a Middle Pleistocene chronology around 450 ka, i.e. significantly younger than the supposedly late Early Pleistocene age of faunal assemblage (see Demuro et al., 2015 and references therein). If it might be possible that fossils were reworked by younger sediment, this chronology nevertheless suggests that Huescár-1 could be chronologically located within the most recent part of the biozone. Moreover, several recent studies state that the specific study of the morphology of the first molars (m1) of *M. Savini* might also potentially provide some indications about the relative age of EVT-7 in comparisons with other sites. As the length and width of the m1 seem to increase during the Pleistocene (Lozano-Fernández et al., 2013a,b) this trend might be used to differentiate the sites. Martínez et al. (2014) compared the m1 of individual adult specimens of this species recovered from EVT-7 at Vallparadís with specimens from other sites like Gran Dolina (Atapuerca), Fuente Nueva 3 and Barranco León D (Orce). Their results suggest that the archaeological level 10 at Vallparadís could be chronostratigraphically correlated with level TD5 at Gran Dolina, having thus an older age than TD-6. However, the magnitude of the metrics errors highlights the existing variability between individuals: despite this slight apparent trend, data from TD4/3, TD-5, TD-6 and EVT-7 are nevertheless all within error (Lozano-Fernández et al., 2013b; Martínez et al., 2014) and can hardly be differentiated from a statistical point of view. Some numerical ages were also tentatively derived from this new approach, but they should be considered with extreme caution since several conceptual and methodological limitations have been recently highlighted by Martin (2014) and Palmqvist et al. (2014).

5. Conclusions

Vallparadís may be considered as an excellent case study showing a good consistency between the ESR ages derived from quartz grains and fossil teeth, suggesting that the faunal assemblage is contemporaneous with the sedimentary matrix. The new results obtained on quartz samples helped to refine the chronology of EVT-8 to 849 ± 48 ka. The main archaeological layer located within EVT-7 yielded a mean ESR age of 858 ± 87 ka, in overall good agreement with magneto-biostratigraphic data, even though it might raise some new questions regarding the chronology of the transition from the Epivillafranchian to the Galerian faunal complex. This new ESR chronology confirms the attribution of Vallparadís to the post-Jaramillo period, probably close to Atapuerca Gran Dolina TD-6 (Atapuerca). From the ESR dating point of view, both sites cannot be chronologically distinguished.

From a methodological perspective, these ESR results illustrate the potential, as well as some of the actual limitations, of the ESR method to date late Early Pleistocene sites. ESR dating of quartz grains based on a standard MAA procedure may provide accurate age estimates, with a precision between 5 and 10% at 1 sigma as soon as the ESR dose reconstruction is carried out under controlled experimental conditions to ensure good fitting of the dose response curves. This site would be an excellent opportunity to test new approaches in the future, such as the regenerative dose procedure, which is significantly less time consuming than the MAA and could potentially provide a better precision on the D_E value. The Ti signal was tentatively measured on the four samples following the "multiple center" approach suggested by Toyoda et al. (2000), but the intensity was too low to get meaningful values for three of them (EVTQ-2, EVTQ-3 and EVTQ-4). An ESR dose response curve was obtained for sample EVTQ-0601, but the fitting was not good enough ($r^2 < 0.95$) to obtain a reliable D_E value.

Combined US-ESR results obtained on fossil teeth showed that this approach can be used in routine up to ~0.8 Ma, in agreement with the work performed by Falguères et al. (1999) at Gran Dolina. However, the role of dental tissue in the dose rate reconstruction is especially crucial for such old samples. In that regard, among the avenues worth exploring in the future, the development and combination of high resolution ESR and U-series analyses of dental tissues seem now a necessary step to improve the accuracy of the age results and to push further the limits of the method.

Acknowledgements

This study was partially sponsored by the project CGL2010-16821 from the Spanish Ministry of Science and Innovation. The Ile-de-France Region Council provided a financial contribution to purchase the ESR spectrometer for the Department of Prehistory, National Museum of Natural History, Paris. LA-ICP-MS U-series analysis were performed at RSES by MD during a research stay funded by a José Castillejo Mobility Fellowship CAS12/00251 from the Spanish Ministry for Education, Culture and Sport. MD is grateful to Carlos Saiz, CENIEH, for his help in an early stage of tooth sample preparation. MD and RG thank Les Kinsley, RSES, for his invaluable support in the LA-ICP-MS U-series acquisition. We also thank Norbert Mercier, University of Bordeaux for providing the gamma dose rate from the TL dosimeters. MD would like to thank Gloria Cuenca Bescos for fruitful discussions and helpful advice about the biochronology based on rodents. Finally, the comments made by the Guest Editor Lee Arnold and two anonymous reviewers contributed to improve the manuscript.

References

Arnold, L.J., Demuro, M., Parés, J.M., Pérez-González, A., Arsuaga, J.L., Bermúdez de Castro, J.M., Carbonell, E., 2015. Evaluating the suitability of extended-range luminescence dating techniques over Early and Middle Pleistocene time-scales: published datasets and case studies from Atapuerca, Spain. Quaternary International 389, 167–190.

Bahain, J.-J., Yokoyama, Y., Falguères, C., Sarcia, M.N., 1992. ESR dating of tooth enamel: a comparison with K–Ar dating. Quaternary Science Reviews 11, 245–250.

Bahain, J.-J., Falguères, C., Voinchet, P., Duval, M., Dolo, J.-M., Despriée, J., Garcia, T., Tissoux, H., 2007. Electron spin resonance (ESR) dating of some European late Lower Pleistocene sites. Quaternaire 18, 175–186.

Bon, M., Piccoli, G., Sala, B., 1992. La fauna pleistocenica delia breccia di Slivia (Carso Triestino) nella collezione del Museo civico di Storia naturale di Trieste. Atti del museo civico di storia naturale di Trieste 44, 33–51.

Brennan, B.J., 2003. Beta doses to spherical grains. Radiation Measurements 37, 299–303.

Brennan, B.J., Lyons, R.G., Phillips, S.W., 1991. Attenuation of alpha particle track dose for spherical grains. Nuclear Tracks and Radiation Measurements 18, 249–253.

Brennan, B.J., Rink, W.J., McGuirl, E.L., Schwarcz, H.P., Prestwich, W.V., 1997. Beta doses in tooth enamel by 'one-group' theory and the ROSY ESR dating software. Radiation Measurements 27 (2), 307–314.

Carbonell, E., Bermudez de Castro, J.M., Pares, J.M., Perez-Gonzalez, A., Cuenca-Bescos, G., Olle, A., Mosquera, M., Huguet, R., van der Made, J., Rosas, A., Sala, R., Vallverdu, J., Garcia, N., Granger, D.E., Martinon-Torres, M., Rodriguez, X.P., Stock, G.M., Verges, J.M., Allue, E., Burjachs, F., Caceres, I., Canals, A., Benito, A., Diez, C., Lozano, M., Mateos, A., Navazo, M., Rodriguez, J., Rosell, J., Arsuaga, J.L., 2008. The first hominin of Europe. Nature 452, 465–469.

Coltorti, M., Albianelli, A., Bertini, A., Ficcarelli, G., Laurenzi, M.A., Napoleone, G., Torre, D., 1998. The Colle Curti mammal site in the Colfiorito area (Umbria-Marchean Apennine, Italy): geomorphology, stratigraphy, paleomagnetism and palynology. Quaternary International 47–48, 107–116.

Cuenca-Bescós, G., Rofes, J., López-García, J.M., Blain, H.-A., De Marfá, R.J., Galindo-Pellicena, M.A., Bennásar-Serra, M.L., Melero-Rubio, M., Arsuaga, J.L., Bermúdez de Castro, J.M., Carbonell, E., 2010. Biochronology of Spanish Quaternary small vertebrate faunas. Quaternary International 212, 109–119.

Cuenca-Bescós, G., López-García, J.M., Galindo-Pellicena, M.A., García-Perea, R., Gisbert, J., Rofes, J., Ventura, J., 2013. The Pleistocene history of Iberomys, an endangered endemic rodent from South Western Europe. Integrative Zoology. http://dx.doi.org/10.1111/1749-4877.12053.

Demuro, M., Arnold, L.J., Parés, J.M., Sala, R., 2015. Extended-range luminescence chronologies suggest potentially complex bone accumulation histories at the Early-to-Middle Pleistocene palaeontological site Huéscar-1 (Guadix-Baza basin, Spain). Quaternary International 389, 191–212.

Duval, M., 2012. Dose response curve of the ESR signal of the aluminum center in quartz grains extracted from sediment. Ancient TL 30 (2), 1–9.

Duval, M., Guilarte Moreno, V., 2012. Assessing the influence of the cavity temperature on the ESR signal of the aluminum center in quartz grains extracted from sediment. Ancient TL 30 (2), 11–16.

Duval, M., Moreno, D., Shao, Q., Voinchet, P., Falguères, C., Bahain, J.-J., Garcia, T., Garcia, J., Martinez, K., 2011a. Datación por ESR del yacimiento arqueológico del Pleistoceno inferior de Vallparadís (Terrassa, Cataluña, España). Trabajos de Prehistoria 68, 7–23.

Duval, M., Aubert, M., Hellstrom, J., Grün, R., 2011b. High resolution LA-ICP-MS mapping of U and Th isotopes in an early Pleistocene equid tooth from Fuente Nueva-3 (Orce, Andalusia, Spain). Quaternary Geochronology 6 (5), 458–467.

Duval, M., Falguères, C., Bahain, J.-J., 2012. Age of the oldest hominin settlements in Spain: contribution of the combined U-series/ESR dating method applied to fossil teeth. Quaternary Geochronology 10, 412–417.

Duval, M., Guilarte Moreno, V., Grün, R., 2013. ESR dosimetry of fossil enamel: some comments about measurement precision, long-term signal fading and dose–response curve fitting. Radiation Protection Dosimetry 157 (4), 463–476.

Echassoux, A., 2004. Étude taphonomique, paléoécologique et archéozoologique des faunes de grands mammifères de la seconde moitié du Pléistocène inférieur de la grotte du Vallonnet (Roquebrune-Cap-Martin, Alpes-Maritimes, France). L'Anthropologie 108 (1), 11–53.

Eggins, S., Grün, R., Pike, A., Shelley, A., Taylor, L., 2003. ^{238}U, ^{232}Th profiling and U-series isotope analysis of fossil teeth by laser ablation ICPMS. Quaternary Science Reviews 22, 1373–1382.

Eggins, S.M., Grün, R., McCulloch, M.T., Pike, A.W.G., Chappell, J., Kinsley, L., Mortimer, G., Shelley, M., Murray-Wallace, C.V., Spötl, C., Taylor, L., 2005. In situ U-series dating by laser-ablation multi-collector ICPMS: new prospects for Quaternary geochronology. Quaternary Science Reviews 24, 2523–2538.

Falguères, C., Bahain, J.-J., Yokoyama, Y., Arsuaga, J.L., Bermudez de Castro, J.M., Carbonell, E., Bischoff, J.L., Dolo, J.-M., 1999. Earliest humans in Europe: the age of TD6 Gran Dolina, Atapuerca, Spain. Journal of Human Evolution 37, 343–352.

Falguères, C., 2003. ESR dating and the human evolution: contribution to the chronology of the earliest humans in Europe. Quaternary Science Reviews 22, 1345–1351.

Gagnepain, J., 1996. Etude Magnetostratigraphique de Sites du Pleistocene Inferieur et Moyen des Alpes-Maritimes et d'Italie: Grotte du Vallonnet, Marina Airport, Ca' Belvedere di Monte Poggiolo, Isernia La Pineta, Venosa, Loreto. Museum National d'Histoire Naturelle, Paris.

Garcia, J., Martínez, K., Carbonell, E., Agustí, J., Burjachs, F., 2012. Defending the early human occupation of Vallparadís (Barcelona, Iberian Peninsula). Journal of Human Evolution 63, 568–575.

Garcia, J., Martínez, K., Carbonell, E., 2013a. The Early Pleistocene stone tools from Vallparadís (Barcelona, Spain): rethinking the European mode 1. Quaternary International 316, 94–114.

Garcia, J., Landeck, G., Martínez, K., Carbonell, E., 2013b. Hominin dispersals from the Jaramillo subchron in central and south-western Europe: Untermassfeld (Germany) and Vallparadís (Spain). Quaternary International 316, 73–93.

Garcia, J., Martínez, K., Cuenca-Bescós, G., Carbonell, E., 2014. Human occupation of Iberia prior to the Jaramillo magnetochron (>1.07 Myr). Quaternary Science Reviews 98, 84–99.

Gliozzi, E., Abbazzi, L., Argenti, P., Azzaroli, A., Caloi, L., Capasso-Barbato, L., Di-Stefano, G., Esu, D., Ficcarelli, G., Girotti, O., Kotsaki, T., Masini, F., Mazza, P., Mezzabotta, C., Paombo, M.R., Petronio, C., Rook, L., Sala, B., Sardella, R., Zanalda, E., Torre, D., 1997. Biochronology of selected mammals, molluscs and ostracods from the Middle Pliocene to the late pleistocene in Italy. The state of the art. Rivista Italiana di Paleontologia e Stratigrafia 103 (3), 369–388.

Gómez Cano, A.R., Hernández Fernández, M., Álvarez-Sierra, M.Á., 2011. Biogeographic provincialism in rodent faunas from the Iberoccitanian Region (southwestern Europe) generates severe diachrony within the Mammalian Neogene (MN) biochronologic scale during the Late Miocene. Palaeogeography, Palaeoclimatology, Palaeoecology 307, 193–204.

Guérin, G., Mercier, N., Adamiec, G., 2011. Dose-rate conversion factors: update. Ancient TL 29 (1), 5–8.

Grün, R., 1994. A cautionary note: use of 'water content' and 'depth for cosmic ray dose rate' in AGE and DATA programs. Ancient TL 12 (2), 50–51.

Grün, R., 1998. Reproducibility measurements for ESR signal intensity and dose determination: high precision but doubtful accuracy. Radiation Measurements 29 (2), 177–193.

Grün, R., Brumby, S., 1994. The assessment of errors in past radiation doses extrapolated from ESR/TL dose-response data. Radiation Measurements 23, 307–315.

Grün, R., Katzenberger-Apel, O., 1994. An alpha irradiator for ESR dating. Ancient TL 12 (2), 35–38.

Grün, R., McDermott, F., 1994. Open system modelling for U-series and ESR dating of teeth. Quaternary Science Reviews 13, 121–125.

Grün, R., Schwarcz, H.P., Chadam, J., 1988. ESR dating of tooth enamel: coupled correction for U-uptake and U-series disequilibrium. International Journal of Radiation Applications and Instrumentation. Part D. Nuclear Tracks and Radiation Measurements 14 (1–2), 237–241.

Grün, R., Eggins, S., Kinsley, L., Moseley, H., Sambridge, M., 2014. Laser ablation U-series analysis of fossil bones and teeth. Palaeogeography, Palaeoclimatology, Palaeoecology. http://dx.doi.org/10.1016/j.palaeo.2014.07.023 (submitted for publication).

Grün, R., Duval, M., 2014. Spatial distribution of U, U-series isotopes and CO2-radicals in tooth enamel. In: Proceedings of the 14th International Conference on Luminescence and Electron Spin Resonance Dating, Montreal (Canada), p. 64.

Grün, R., Huang, P.H., Huang, W., McDermott, F., Stringer, C.B., Thorne, A., Yan, G., 1998. ESR and U-series analyses of teeth from the palaeoanthropological site of Hexian, Anhui Province, China. Journal of Human Evolution 34, 555–564.

Head, M.J., Gibbard, P.L., 2005. Early–Middle Pleistocene transitions: an overview and recommendation for the defining boundary. In: Head, M.J., Gibbard, P.L. (Eds.), Early–Middle Pleistocene Transitions: the Land–Ocean Evidence, Special Publication, Geological Society of London, London, 251, pp. 1–18.

Kahlke, R.D., 2009. Les communautés de grands mammifères du Pléistocène inférieur terminal et le concept d'un biochrone Épivillafranchien. Quaternaire 20, 415–427.
López-García, J.M., Cuenca-Bescós, G., Blain, H.-A., Cáceres, I., García, N., van der Made, J., Gutierrez, J.M., Santiago, A., Pacheco, F.G., 2012. Biochronological data inferred from the Early Pleistocene Arvicolinae (Mammalia, Rodentia) of the El Chaparral Site (Sierra Del Chaparral, Cádiz, Southwestern Spain). Journal of Vertebrate Paleontology 32 (5), 1149–1156.
Lozano-Fernández, I., Cuenca-Bescós, G., Blain, H.-A., López-García, J.M., Agustí, J., 2013a. *Mimomys savini* size evolution in the Early Pleistocene of south-western Europe and possible biochronological implications. Quaternary Science Reviews 76, 96–101.
Lozano-Fernández, I., Agustí, J., Cuenca-Bescós, G., Blain, H.-A., López-García, J.M., Vallverdú, J., 2013b. Pleistocene evolutionary trends in dental morphology of Mimomys savini (Rodentia, Mammalia) from Iberian peninsula and discussion about the origin of the genus Arvicola. Quaternaire 24 (2), 179–190.
Madurell-Malapeira, J., Minwer-Barakat, R., Alba, D.M., Garcés, M., Gómez, M., Aurell-Garrido, J., Ros-Montoya, S., Moyà-Solà, S., Berástegui, X., 2010. The Vallparadís section (Terrassa, Iberian Peninsula) and the latest Villafranchian faunas of Europe. Quaternary Science Reviews 29, 3972–3982.
Martin, R.A., 2012. Victoriamys, a new generic name for Chaline's vole from the Pleistocene of Western Europe. Geobios 45 (5), 445–450.
Martínez, K., Garcia, J., Carbonell, E., Agustí, J., Bahain, J.-J., Blain, H.-A., Burjachs, F., Cáceres, I., Duval, M., Falguères, C., Gómez, M., Huguet, R., 2010. A new Lower Pleistocene archeological site in Europe (Vallparadís, Barcelona, Spain). Proceedings, National Academy of Sciences 107, 5762–5767.
Martínez, K., Garcia, J., Carbonell, E., 2013. Hominin multiple occupations in the Early and Middle Pleistocene sequence of Vallparadís (Barcelona, Spain). Quaternary International 316, 115–122.
Martínez, K., Garcia, J., Burjachs, F., Yll, R., Carbonell, E., 2014. Early human occupation of Iberia: the chronological and palaeoclimatic inferences from Vallparadís (Barcelona, Spain). Quaternary Science Reviews 85, 136–146.
Martin, R.A., 2014. A critique of vole clocks. Quaternary Science Reviews 94, 1–6.
Masini, F., Giannini, T., Abbazzi, L., Fanfani, F., Delfino, M., Christian Maul, L., Torre, D., 2005. A latest Biharian small vertebrate fauna from the lacustrine succession of San Lorenzo (Sant'Arcangelo Basin, Basilicata, Italy). Quaternary International 131, 79–93.
Masini, F., Sala, B., 2007. Large- and small-mammal distribution patterns and chronostratigraphic boundaries from the Late Pliocene to the Middle Pleistocene of the Italian peninsula. Quaternary International 160, 43–56.
Maul, L.C., Markova, A.K., 2007. Similarity and regional differences in Quaternary arvicolid evolution in Central and Eastern Europe. Quaternary International 160, 81–99.
Minwer-Barakat, R., Madurell-Malapeira, J., Alba, D.M., Aurell-Garrido, J., De Esteban-Trivigno, S., Moyà-Solà, S., 2011. Pleistocene rodents from the Torrent de Vallparadís section (Terrassa, northeastern Spain) and biochronological implications. Journal of Vertebrate Paleontology 31, 849–865.
Muttoni, G., Scardia, G., Kent, D.V., 2013. A critique of evidence for human occupation of Europe older than the Jaramillo subchron (~1 Ma): comment on 'The oldest human fossil in Europe from Orce (Spain)'. Journal of Human Evolution 65, 746–749.
Palmqvist, P., González-Donoso, J.M., De Renzi, M., 2014. Rectilinear evolution in arvicoline rodents and numerical dating of Iberian Early Pleistocene sites. Quaternary Science Reviews 98, 100–109.
Palombo, M.R., 2007. What is the boundary for the Quaternary period and Pleistocene epoch? The contribution of turnover patterns in large mammalian complexes from north-western Mediterranean to the debate. Quaternaire 18 (1).
Parés, J.M., Pérez-González, A., 1999. Magnetochronology and stratigraphy at Gran Dolina section, Atapuerca (Burgos, Spain). Journal of Human Evolution 37, 325–342.
Parés, J.M., Arnold, L., Duval, M., Demuro, M., Pérez-González, A., Bermúdez de Castro, J.M., Carbonell, E., Arsuaga, J.L., 2013a. Reassessing the age of Atapuerca-TD6 (Spain): new paleomagnetic results. Journal of Archaeological Science 40, 4586–4595.
Parés, J.M., Duval, M., Arnold, L.J., 2013b. New views on an old move: hominin migration into Eurasia. Quaternary International 295, 5–12.
Paunescu, A.-C., 2001. Les rongeurs du Pléistocène inférieur et moyen de trois grottes du Sud-Est de la France (Vallonnet, Caune de l'Arago, Baume Bonne). Implications systématiques, biostratigraphiques et paléoenvironnementales (PhD thesis). Muséum national d'Histoire naturelle, Paris.
Petronio, C., Sardella, R., 1999. Biochronology of the Pleistocene mammal from Ponte Galeria (Rome) and remarks on the middle fauna from Galerian faunas. Rivista Italiana di Paleontologia e Stratigrafia 1, 155–164.
Pickering, R., Jacobs, Z., Herries, A.I.R., Karkanas, P., Bar-Matthews, M., Woodhead, J.D., Kappen, P., Fisher, E., Marean, C.W., 2013. Paleoanthropologically significant South African sea caves dated to 1.1–1.0 million years using a combination of U–Pb, TT-OSL and palaeomagnetism. Quaternary Science Reviews 65, 39–52.
Prescott, J.R., Hutton, J.T., 1994. Cosmic ray contributions to dose rates for luminescence and ESR dating: large depths and long-term time variations. Radiation Measurements 23, 497–500.
Rhodes, E.J., Singarayer, J.S., Raynal, J.P., Westaway, K.E., Sbihi-Alaoui, F.Z., 2006. New age estimates for the Palaeolithic assemblages and Pleistocene succession of Casablanca, Morocco. Quaternary Science Reviews 25, 2569–2585.
Rook, L., Martínez-Navarro, B., 2010. Villafranchian: the long story of a Plio-Pleistocene European large mammal biochronologic unit. Quaternary International 219, 134–144.
Shao, Q., 2011. Combined ESR/U-series Dating of Fossil Teeth from Middle Pleistocene Sites in Northern Europe and Mediterranean Area: Contributing to the Chronology of the Acheulian Settlement of Europe (PhD thesis). Muséum National d'Histoire Naturelle, Paris.
Toro-Moyano, I., Martínez-Navarro, B., Agustí, J., Souday, C., Bermúdez de Castro, J.M., Martinón-Torres, M., Fajardo, B., Duval, M., Falguères, C., Oms, O., Parés, J.M., Anadón, P., Julià, R., García-Aguilar, J.M., Moigne, A.-M., Espigares, M.P., Ros-Montoya, S., Palmqvist, P., 2013. The oldest human fossil in Europe, from Orce (Spain). Journal of Human Evolution 65 (1), 1–9.
Toyoda, S., Voinchet, P., Falguères, C., Dolo, J.M., Laurent, M., 2000. Bleaching of ESR signals by the sunlight: a laboratory experiment for establishing the ESR dating of sediments. Applied Radiation and Isotopes 52 (5), 1357–1362.
Toyoda, S., Falguères, C., 2003. The method to represent the ESR signal intensity of the aluminium hole center in quartz for the purpose of dating. Advances in ESR Applications 20, 7–10.
Vandenberghe, D., De Corteb, F., Buylaert, J.P., Kucera, J., Van den haute, P., 2008. On the internal radioactivity in quartz. Radiation Measurements 43, 771–775.
Van Kolfschoten, T., Markova, A.K., 2005. Response of the European mammalian fauna to the mid-Pleistocene transition. In: Head, M.J., Gibbard, P.L. (Eds.), Early–Middle Pleistocene Transitions: the Land–Ocean Evidence, Geological Society of London Special Publication, vol. 251, pp. 221–229.
Yokoyama, Y., Nguyen, H.V., 1980. Direct and non destructive dating of marine sediments, manganese nodules and corals by high resolution gamma-ray spectrometry. In: Goldberg, E.D., Horibe, Y., Saruhashi, K., et al. (Eds.), Isotope Marine Chemistry. Uchida Rokakuho, Tokyo, pp. 259–289.
Yokoyama, Y., Falgueres, C., Quaegebeur, J.P., 1985. ESR dating of quartz from Quaternary sediments: first attempt. Nuclear Tracks and Radiation Measurements 10, 921–928.